

# Novel K-Band Prime Focus Reflector-Coupled Focal Plane Array

Lisa S. Locke<sup>1,2</sup>, Jens Bornemann<sup>1</sup> and Stéphane Claude<sup>2</sup>

<sup>1</sup>Department of Electrical Engineering, University of Victoria, Victoria, BC, V8W 3P6, Canada

<sup>2</sup>Herzberg Institute of Astrophysics, National Research Council of Canada, Victoria, BC, V9E 2E7, Canada

**Abstract**—A wideband focal plane array (FPA) covering the full K-band (18 – 26.5 GHz) is proposed for use in passive imaging and microwave astronomy. Focal plane arrays are revolutionizing microwave and millimeter-wave imaging by replacing conventional single-pixel feed horns with arrays of planar elements, decreasing the survey time dramatically. The extent and element spacing of a rectangular array is determined by comparing classic and encircled power techniques. A prime focus reflector-feed configuration is considered with  $f/D=0.45$ . Far-field performances of arrays of simple Gaussian feeds and also imported Vivaldi feeds, which include mutual coupling between elements, are evaluated by PO/PTD techniques.

**Keywords**— Focal plane array; K-band; wideband; prime focus reflector; antipodal Vivaldi antenna; mutual coupling

## I. INTRODUCTION

A focal plane array, also called “dense focal plane array” [1] or “array feed”, is defined as a dense array of feeds at the focus of a reflector, effectively creating a multi-pixel camera. The feed elements map multiple beams on the sky, increasing the field of view. Conventionally, this has been realized with clusters of waveguide horns forming non-contiguous beams on the sky as large horn diameters of  $2-3\lambda$  prevent dense placement at the focus [2]. The spatial gaps in imaging require multiple passes across the view, thus longer imaging times. However, focal plane array elements can be placed much closer,  $0.5\lambda$ , to create multiple overlapping beams simultaneously, effectively sampling the focal plane and improving the survey speed dramatically [3]. Other benefits of beamformed focal plane arrays include interference cancellation [4], correction of reflector surface defects [5] and the ability to produce specific radiation patterns used by geostationary satellites [6].

Currently there are several L-band (1-2 GHz) focal plane array systems developed for imaging and microwave astronomy [7-11]. K-band includes molecular transitions of ammonia and a  $\text{HC}_7\text{N}$  line. We present the design of an 18 - 26.5 GHz focal plane array of planar Vivaldi feeds as a technology demonstrator for high frequency planar feed arrays.

This paper is organized as follows: an overview of the single Vivaldi element in Section 2. Element spacing and maximum array size determination using classical optical methods and the encircled power method [12] in Section 3. Section 4 shows the performance of 6.2 mm- and 12.4 mm-pitch (element separation)  $5\times 5$  and  $15\times 15$  arrays of Gaussian feeds, calculating secondary far-field characteristics. Cross-

over levels between far field beams verify the geometrical parameters calculated in Section 3. Section 5 incorporates the effects of mutual coupling between Vivaldi elements determined from a full-wave solution of the  $5\times 5$  array and computes the far-field secondary radiation characteristics. The relative gain and beam quality of three feed elements are evaluated along a diagonal from the center pixel.

## II. INDIVIDUAL ANTENNA ELEMENT

The planar end-fire Vivaldi element [13] is an excellent choice for wide-band, compact, highly directive applications that require axially symmetric beams [14]. The Vivaldi element used in this paper is based on a previous design [15] of an 18-30 GHz, 11 mm,  $0.9\lambda$  wide antipodal linear tapered slot antenna but with a reduced aperture width of 6.2 mm ( $0.5\lambda$ ). The antenna is substrate integrated waveguide (SIW) fed on a high dielectric Rogers/Duroid 6010 substrate ( $\epsilon_r=10.2$ ) required for minimal spacing between antenna array elements. The SIW equivalent waveguide is 3.14 mm with a  $\text{TE}_{10}$ -mode cutoff of 15.1 GHz, offering single-mode propagation up to the  $\text{TE}_{20}$  mode cutoff of 30.2 GHz [16]. The antipodal configuration is often used in combination with SIW structures as the electric field vector rotates in phase through  $90^\circ$  from antenna aperture to SIW section. Poor cross-polarization reported [17] in Vivaldi-type antennas due to non-zero transverse distance between top and bottom metal conductors has been combated with edge corrugations [18].

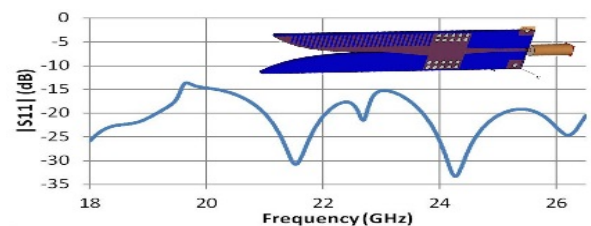


Fig. 1. Input return loss (dB) of single Vivaldi element.

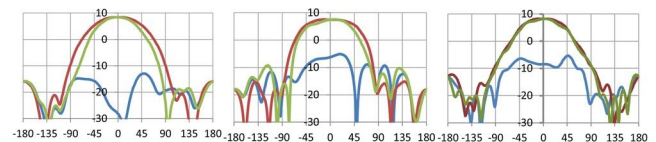


Fig. 2. Single element far-field directivity (dBi) vs  $\theta$  (degrees) for principle planes at 18, 22, and 26 GHz (left to right). Red:  $H_{\text{copol}}$  ( $\phi=0^\circ$ ), green:  $E_{\text{copol}}$  ( $\phi=90^\circ$ ), blue:  $D_{\text{xpol}}$  ( $\phi=45^\circ$ ). Ludwig's 3<sup>rd</sup> definition of cross-polarization is used. HPBW for E/H at 18, 22, 26 GHz:  $68/90^\circ$ ,  $81/104^\circ$ ,  $72/85^\circ$ .

The individual Vivaldi element is presented in Figs. 1 and 2. The return loss is better than -14 dB, directivity varies 8-9

The authors would like to acknowledge support of this work from the National Science and Engineering Research Council of Canada.

dB, far-field patterns are highly symmetric in E- and H- planes and low cross-polarization despite the narrow  $\lambda/2$  width.

### III. ARRAY GEOMETRY

An array is defined by the individual element pattern, the relative spacing between elements, and geometrical layout including maximum extent.

#### A. Element Spacing

To avoid grating lobes the maximum element spacing  $d$  ( $\lambda$ ) for an array at the focus of a reflector of half angle  $\theta$ , is [19]

$$d/\lambda = (1 + \sin \theta)^{-1} \quad (1)$$

For a nominal  $f/D$  of 0.45, the half angle is  $\theta = 58^\circ$ ; therefore, the element spacing in both x- and y-planes is  $d = 6.2$  mm.

#### B. Geometrical Layout Including Maximum Extent

A planar array using a rectangular xy-grid is used. The y-spacing is along the substrate and the x-spacing is between separate substrate “boards”.

Classical work on paraboloidal reflectors can be used to estimate the maximum radial feed dimension,  $\rho/\lambda$ , determined by the location off of focus where the axial distance between the flat array and the curved focal arc differs within a given margin of error as shown in Fig. 4 of [20]. For operating wavelength  $\lambda_{max}=16.7$  mm and the previously mentioned reflector, the maximum extent between the paraboloid focus and the edge,  $r_{0max}$ , is:

$$r_{0max} = 2f / (1 + \cos \theta) = 5.88 \text{ m} \quad (2)$$

Calculate the radial dimension  $\rho$  of the feed in the focal plane:

$$\rho \leq 0.35\sqrt{(r_{0max} \lambda)} = 91 \text{ mm} = 5.5\lambda_{max} \quad (3)$$

The largest square array circumscribed in a circle with radius  $\rho$  is  $\rho/\sqrt{2} = 129$  mm x 129 mm. Since phased array feeds utilize additional beamforming, which decrease aberrations off axis,  $\rho$  represents a conservative limit.

Secondly, for reflector systems, from [12] the encircled power in the focal region is calculated as a function of focal plane radius,  $f/D$  ratio and reflector diameter. The focal plane radius for a reflector of  $f/D = 0.45$ , is 40.5 mm at 79 percent encircled power. This corresponds to a maximum array size of 71mm x 71 mm.

We propose a 5x5 K-band array at element spacing 6.2 mm x 6.2 mm for an overall size of 31 mm x 31 mm with the future possibility of using this building block as a subset of a larger 15x15 array, a maximum size of 93 mm x 93 mm. The 5x5 array is well within the most conservative maximum array size limit set forth by the encircled power method and the 15x15 array size is within the classical radius calculation limit. At this moment however, the maximum array size is set not by the optics of the reflector and feed system but rather by the receiver expense and required signal processing systems.

### IV. IDEAL GAUSSIAN FEEDS

To verify the estimated array separation and focal plane array extent, the relative gain drop and distortion in the far field

of the outermost beams is analyzed. We simulate a 5x5 array and an extended 15x15 array at the recommended pitch 6.2 mm and a 100% increased pitch 12.4 mm. The  $f/D=0.45$  prime focus 10 m diameter reflector feed configuration described in Section 3 is retained.

The simulations are performed using the physical optics and physical theory of diffraction (PO/PTD) techniques in GRASP10 from TICRA. This software offers a pattern defined, far field Gaussian beam object class, setting the frequency, taper angle and taper value for a far field radiated Gaussian beam. While using this object for the feed array does not account for the mutual coupling between feeds, this is a logical preliminary step to validate the element separation and extent. Each feed is defined with a 3 dB edge taper at half angle  $\theta = 58^\circ$  at midband, 22 GHz, in order to ensure maximum illumination of the reflector. We recognize that excess noise will be introduced due to the shallow taper; optimizing spillover efficiency will be presented in future work.

#### A. 6.2mm Element Separation – 5x5 and 15x15

The far field radiation patterns of each feed within the array are defined as primary beam patterns. The far field radiation patterns of the feed-reflector combination are denoted the secondary beam patterns. Fig. 3 shows the secondary beam patterns for a 5x5 array with 6.2 mm pitch. The raster image is the composite image formed by the complex addition of all 5x5 far-field element beams, each centered at the crosses, each weighted equally in amplitude and phase. Only the co-polar results are shown of these ideal feeds.

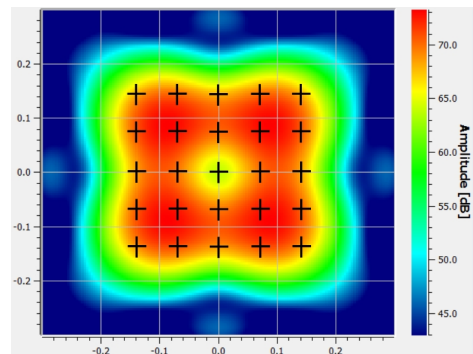


Fig. 3. Secondary beam patterns of 5x5 array of ideal Gaussian feeds centered at crosses at 6.2 mm pitch, 22 GHz, amplitude is co-polar gain (dB). Composite pattern obtained by complex addition of all individual beams weighted equally in amplitude and phase. X: azimuth ( $^\circ$ ). Y: elevation ( $^\circ$ ).

There is a  $\sim 9$  dB dip at the center of the composite beam, which can be minimized by adjusting the relative amplitude weightings. Fig. 4 shows the secondary beam pattern for both 5x5 (solid lines) and an extended 15x15 (dotted lines) array. A cut-plane through the center row of the array identifies individual element patterns before complex addition and element weighting. The results show a maximum gain drop at the edge of the 5x5 array of only 0.2 dB, and at the edge of the 15x15 array is -1.5 dB. We can infer that the 15x15 array will perform adequately if the gain drop can be tolerated, and from

Fig. 4 some amplitude tapering should be employed to improve gain flatness across the field of view.

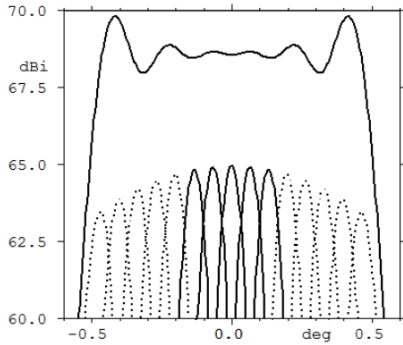


Fig. 4. Secondary beam patterns of 5x5 (solid) and 15x15 (dotted) arrays of ideal Gaussian feeds at 6.2 mm pitch, 22 GHz, co-polar gain (dB) vs azimuth (deg). Cut-plane of element patterns through array center of each beam before complex addition. Cross-over level between beams is 63.2 dB.

### B. 12.2mm Element Separation – 5x5 and 15x15

Doubling the distance between feed elements to 12.4 mm results in poor field of view coverage seen in Fig. 5 in the composite secondary beam patterns for a 5x5 array with pitch 12.4 mm. The peak gain is ~ 8 dB below that of the maximum of Fig. 3’s properly spaced (6.2 mm) elements. Fig 6 shows the secondary beam patterns along a cut plane through the center row for both 5x5 and an extended 15x15 array. A maximum gain drop at the edge of 5x5 array of -0.6d dB and at the edge of the 15x15 array of -5.8 dB. The beam overlap level is well below 6 dB relative to the center element. The 12.4 mm spacing is not recommended due to the low-gain results and sparse field of view.

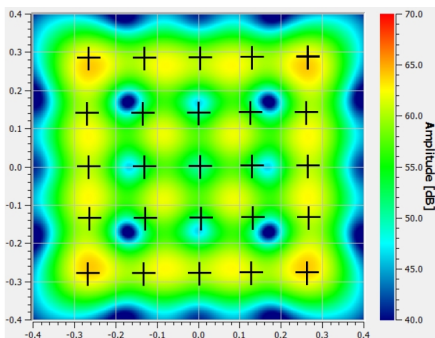


Fig. 5. Secondary beam patterns of 5x5 array of ideal Gaussian feeds centered at crosses at 12.4 mm pitch, 22 GHz, amplitude is co-polar gain (dB). Composite pattern obtained by complex addition of individual beams weighted equally in amplitude and phase. X: azimuth (°). Y: elevation (°).

### V. IMPORTED VIVALDI FEEDS WITH MUTUAL COUPLING

Mutual coupling between the Vivaldi elements of the 5x5 array is now taken into account by using a full-wave finite element analysis EM simulator, Ansoft HFSS, to calculate each far-field primary beam and the simultaneous mutual coupling of all other beams. These far fields are imported into GRASP and the secondary beam patterns including the reflector are calculated. The resulting secondary co-polar and cross-polar radiation patterns taking into account the mutual coupling of the beams are shown in Fig. 7 and the beams are defined as center (0°, 0°), mid (0.675°, 0.675°), and upper-right (0.135°, 0.135°). The center element at the focus shows a

well-formed co-polar beam and low (-19 dB) cross-polar levels. The upper-right beam displays a small amount of distortion with moderate (-13 dB) cross-polar levels.

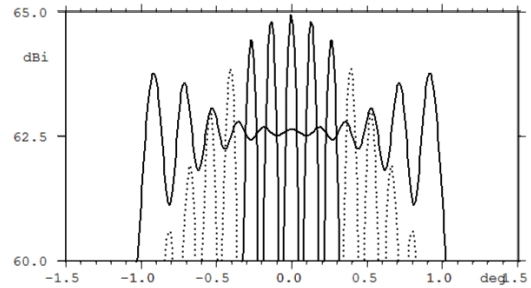


Fig. 6. Secondary beam patterns of 5x5 (solid) and 15x15 (dotted) arrays of ideal Gaussian feeds at 12.4 mm pitch, 22 GHz, co-polar gain (dB) vs azimuth (°). Cut-plane of element patterns through array center of each beam before complex addition.

The individual elements’ co-polar gains of Fig. 7 are displayed as superimposed contours in Fig. 8 to show the overlapping levels between the beams. These diagonal elements which are farther apart than along rows or columns of elements and thus present the worst case for element overlap. The center and mid beams overlap at -3.29 dB from center beam’s peak. The mid and upper-right beams overlap at -2.94dB and -4.91 dB relative to mid and upper-right beam peaks respectively. The gain differentials and aberrations of the most out-of-focus, the upper right beam, are acceptable and prove the efficacy of this array configuration.

### VI. CONCLUSIONS

A K-band 5x5 focal plane array with planar Vivaldi elements spaced 6.2 mm is presented for use in conjunction with a 10 m, 0.45  $f/D$  prime focus reflector for astronomy and general imaging applications. Classical optics and encircled-power methods are used to determine maximum array size and are verified using simulations with Gaussian feed elements on a reflector-array configuration showing overlapping beam levels and aberrations. Mutual coupling effects are incorporated by importing full-wave solver far fields for the Vivaldi elements and using PO/PTD techniques to calculate the secondary far fields with the reflector and feed combination. The performance of a 6.2 mm pitch 5x5 K-band focal plane array and the array - prime focus reflector configuration is thus validated.

### REFERENCES

- [1] M. Ivashina, M. Kehn, P.-S. Kildal, and R. Maaskant, “Decoupling efficiency of a wideband Vivaldi focal plane array feeding a reflector antenna,” *IEEE Trans. Antennas Propagat.*, vol. 57, pp. 373-382, Feb. 2009.
- [2] J. Johansson, “Fundamental limits for focal-plane array efficiency,” in *Multi-Feed Systems for Radio Telescopes*, ser. *Astron. Soc. Pac. Conf.*, vol. 75, Tucson, USA, pp. 34-41, May 1994.
- [3] B. Veidt, “Focal-plane array architectures: Horn clusters vs. phase-array techniques,” *International Square Kilometre Array Steering Committee*, SKA Memo 71, 2006.
- [4] B.D. Jeffs, K.F. Warnick, J. Landon, J. Waldron, D. Jones, J.R. Fisher, and R.D. Norrod, “Signal processing for phased array feeds in radio astronomical telescopes,” *IEEE J. Sel. Topics Signal Process.*, vol. 2, no. 5, pp. 635-646, Oct. 2008.

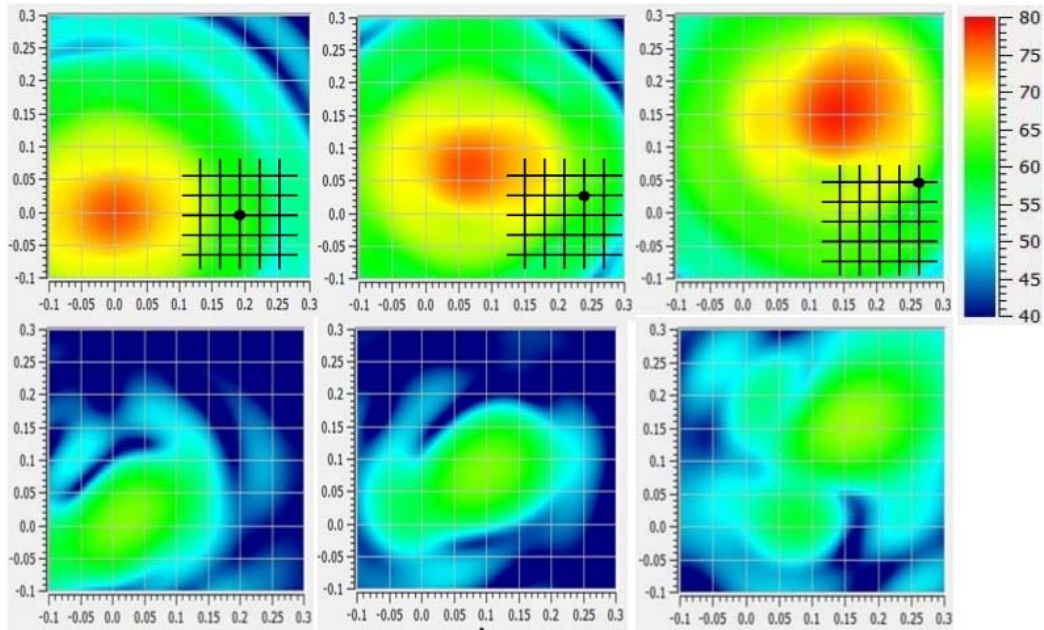


Fig. 7. Secondary beam characteristics of center, mid and upper right elements as shown in inset of 5x5 array of Vivaldi feeds including mutual coupling, composite image. Left/middle/right columns: center/mid/upper right beams as depicted in inset. Top row: Co-polarized gain (dB) of element only. Bottom row: Cross-polarized gain (dB) of element only. X: azimuth ( $^{\circ}$ ). Y: elevation ( $^{\circ}$ ). 22 GHz

- [5] W. Smith and W. Stutzman, "A pattern synthesis technique for array feeds to improve radiation performance of large distorted reflector antennas," *IEEE Trans. Antennas Propagat.*, vol. 40, pp. 57-62, Jan. 1992.
- [6] W. Williams and J. Howell, "Communications satellite antennas with on-orbit pattern flexibility," *Microw. J.*, vol. 8, pp. 22-43, Aug. 2004.
- [7] P. Dewdney, P. Hall, R. Schilizzi, and T. Lazio, "The square kilometre array", *Proc. IEEE*, vol. 97, pp. 1482-1496, Aug. 2009.
- [8] K.F. Warnick, B.D. Jeffs, J. Landon, J. Waldron, D. Jones, J.R. Fisher, and R. Norrod, "Beamforming and imaging with the BYU/NRAO L-band 19-element phased array feed," *Proc. ANTEM/URSI*, pp. 1-4, Banff, Canada, Feb. 2009.
- [9] M. Arts, M. Ivashina, O. Iupikov, L. Bakker, and R. van den Brink, "Design of a low-loss low-noise tapered slot phased array feed for reflector antennas," *Proc European Conf. Antennas Propagat.*, pp. 1-5, Barcelona, Spain, Apr. 2010.
- [10] B. Veidt, G.J. Hovey, T. Burgess, R.J. Smegal, R. Messing, A.G. Willis, A.D. Gray, and P.E. Dewdney, "Demonstration of a dual-polarized phased-array feed," *IEEE Trans. Antennas Propagat.*, vol. 59, pp. 2047-2057, June 2011.
- [11] D.R. DeBoer, R.G. Gough, J.D. Bunton, T.J. Cornwell, R.J. Beresford, . Johnston, I.J. Feain, A.E. Schinckel, C.A. Jackson, M.J. Kesteven, A. Chippendale, G.A. Hampson, J.D. O'Sullivan, S.G. Hay, C.E. Jacka, T.W. Sweetnam, M.C. Storey, L. Ball, and B.J. Boyle, "Australian SKA pathfinder: A high-dynamic range wide-field of view survey telescope," *Proc. IEEE*, vol. 97, pp. 1507-1521, Aug. 2009.
- [12] D. Hayman, T. Bird, K. Esselle, and P. Hall, "Encircled power study of focal plane field for estimating focal plane array size," *IEEE AP-S Int. Symp. Dig.*, vol. 3A, Washington, USA, pp. 371-374, July 2005.
- [13] P. Gibson, "The Vivaldi aerial", *Proc. 9<sup>th</sup> European Microwave Conf.*, pp. 101-105, Brighton, UK, Sep. 1979.
- [14] K. Yngvesson, D. Schaubert, T. Korzeniowski, E. Kollberg, T. Thungren, and J. Johansson, "Endfire tapered slot antennas on dielectric substrates," *IEEE Trans. Antennas Propagat.*, vol. 33, pp. 1392-1400, Dec. 1985.
- [15] L. Locke, J. Bornemann, and S. Claude, "Substrate integrated waveguide-fed tapered slot antenna with smooth performance characteristics over an ultra-wide bandwidth", *Applied Computational Electromagnetics Society (ACES) Journal*, vol. 28, no. 5, pp. 454-462, May 2013.
- [16] D. Deslandes and K. Wu, "Integrated microstrip and regular waveguide in planar form," *IEEE Microwave Wireless Comp. Lett.*, vol. 11, pp. 68-70, Feb. 2001.
- [17] N. Fourikis, N. Lioutas, and N. Shuley, "Parametric study of the co- and crosspolarisation characteristics of tapered planar and antipodal slotline antennas," *IEE Proc. Microw. Antennas Propag.*, vol. 140, pp. 17-22, Feb. 1993.
- [18] H. Sato, Y. Takagi, and K. Sawaya, "High gain antipodal Fermi antenna with low cross polarization," *IEICE Trans. Commun.*, vol. E94-B, pp. 2292-2297, Aug. 2011.
- [19] J. Fisher and R. Bradley, "Full-sampling focal plane arrays," in *Imaging at Radio through Submillimeter Wavelengths*, *Astron. Soc. Pac. Conf.*, J. G. Mangum and S. J. E. Radford, Eds., vol. 217, pp. 11-18, 2000.
- [20] H. Minnett and B. MacA. Thomas, "Fields in the image space of symmetrical focusing reflectors", *Proc. IEE*, vol. 115, pp. 1419-1430, Oct. 1968.

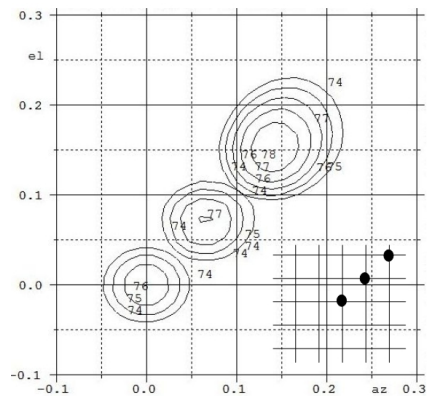


Fig. 8. Secondary beam characteristics of center, mid and upper right elements as shown in inset of 5x5 array of Vivaldi elements including mutual coupling. Contours of co-polar gain (dB) of individual element patterns of center, mid and upper right elements as shown in Fig 7. Gain contour levels as shown. X: azimuth ( $^{\circ}$ ). Y: elevation ( $^{\circ}$ ).